

Enhanced Numerical Simulation and Experimental Validation of Dam Gate Trunnion Rod Anchorage Systems Under Varied Pre-Tensioning Conditions

Wael Zatar, Hien Nghiem, Jason Ray and Brian Eick

ABSTRACT

This research presents a comprehensive Finite Element Analysis (FEA) approach to verify the testing configuration for trunnion rod anchorage assemblies used in dam gates, considering their relevant in-situ conditions. A substantial number of Finite Element (FE) models were constructed using Abaqus/CAE 2023, focusing on the effects of varying pre-tension levels and potential failure modes of trunnion rods. One hundred ninety-seven distinct models were developed, each capturing various rod failure configurations and pre-tensioning scenarios, while consistently maintaining the geometric, mesh, and assembly configurations across the different test cases. To enhance efficiency and ensure consistent testing across a wide range of configurations, a Python script was created to automate the model generation process. The resulting test plan comprised 57 configurations at a pre-stressing level of 15%, in addition to 35 configurations corresponding to pre-stressing levels of 30%, 40%, 50%, and 60% of the Guaranteed Ultimate Tensile Strength. A comparative analysis between the FEA simulations and experimental laboratory tests revealed a mean absolute percentage difference of 6.86% for the initial post-tension levels. The final post-tension levels obtained from the FEA simulations showed a mean absolute percentage difference of 10.99% compared to the laboratory results. The impact of the applied load is more pronounced at lower post-tension levels, particularly at 15%. In contrast, at a 60% post-tension level, the influence of the applied actuator load appears minimal compared to the significant effects noted at the 15% post-tension level. The most substantial differences in tension levels between the laboratory testing and the FEA models primarily occur at the 15% pre-stressing level. These results confirm the reliability of the FEA models in predicting the structural behavior of trunnion rod anchorage assemblies, paving the way for future assessments of the remaining life of these assemblies.

Wael Zatar, Marshall University, Huntington, WV 25755, U.S.A.

Hien Nghiem, Marshall University Research Corporation, Huntington, WV 25755, U.S.A.

Jason Ray, U.S. Army Engineer Research and Development Center, Vicksburg, MS 39183.

Brian Eick, U.S. Army Construction Engineering Research Lab, Champaign, IL 61822, U.S.A.

INTRODUCTION

The United States Army Corps of Engineers (USACE) manages an extensive portfolio of dams equipped with Tainter gates, which are widely regarded as one of the most effective gate types for regulating dam spillways. Post-tensioned anchorage systems are commonly used in these gates, particularly in regions with high dam densities such as the Mississippi Valley Division, Great Lakes and Rivers Division, Southwestern Division, and Northwestern Division.

Between 2010 and 2017, testing of ten dams across the United States revealed major maintenance challenges and opportunities for performance improvement. Eight of these dams exhibited failures in their post-tensioned trunnion rods. A thorough evaluation of 5,371 greased trunnion post-tensioned rods uncovered 22 instances of breakage and six cases of slipping gripping hardware. Additionally, the Markland Dam and the Greenup Dam faced critical issues, with 202 rods on the Markland Dam and 76 rods on the Greenup Dam showing substantial cantilever bending or corrosion. Addressing these issues is crucial to preventing further failures in the post-tensioned trunnion systems.

O'Donnell [1] outlined design considerations for prestressed concrete anchorages supporting Tainter gates. The initial post-tension force applied immediately after anchorage seating should not exceed 70% of the steel's ultimate strength to accommodate losses in steel stress from elastic shortening, creep, and plastic flow.

A case study by Abela and Abela [2] assessed the capacity of the structural members of an existing trunnion girder using an FE model. It investigated the likelihood of a critical anchor failure using non-destructive dispersive wave propagation testing and load testing data of similar anchors at other dams. The results indicated a higher-than-expected probability of critical anchor failure and suggested that a significant flood event could compromise the post-tensioned anchorage system. As a response, the authors proposed two mitigation strategies.

Additionally, Abela [3] assessed the adequacy of a passive anchorage system under increased hydrostatic loading through FE analysis and existing structural and mechanical design manuals. This study emphasized several key factors for evaluating an existing passive anchorage system. These include analyzing the behavior of the anchorage system with FE models, considering Von Mises's stress and elongation of the system, understanding both historical and current codified guidelines, applying the correct classification, and accounting for corrosion of embedded anchors.

Malik and Zatar [4, 5] focused on structural health monitoring approaches to support waterway infrastructure. Nguyen et al. [6] and Zatar et al. [7, 8] reported successful methods for analytical and non-destructive testing of concrete structures. Additionally, Zatar et al. [9] developed FE simulations for six different configurations of trunnion failure scenarios. The FE simulations' results accurately predicted the load changes on each rod under various loads and de-tensioning configurations. These findings provide valuable insights into anchor rod failure rates, allowing engineers assess the current condition of anchor rods and plan proactive maintenance and remediation strategies.

The research team performed NDT laboratory testing and FE analyses on a scaled model of a Tainter gate used in navigation dams using Abaqus/CAE 2023 to assess force distribution and evaluate the increased forces experienced by the remaining post-tensioned trunnion rods resulting from the failure of one to three of these rods.

SCALED MODEL OF THE TAINTER GATE STRUCTURE

This study aims to investigate the impact of one or more trunnion rod failures on the surrounding trunnion rods. The test configuration consists of a large reinforced concrete trunnion beam supported by a series of steel framing. The steel frame was accurately modeled and analyzed following AISC-LRFD [10] standards. The steel components were fabricated, and fit-up was conducted on-site.

The reinforced concrete beam features nine trunnion rods arranged in a three-by-three grid. This beam is designed to simulate the concrete pier of a dam and is anchored to the strong floor with threaded rods to ensure stability. The test configuration was tailored to fit the laboratory space, utilizing the strong floor for anchoring the reinforced concrete beam and an adjacent strong wall to secure two identical actuators that would apply the load. Each trunnion rod is outfitted with a load cell fixed at its dead end to monitor tension throughout the testing process.

The reinforced concrete beam features nine trunnion rods arranged in a three-by-three grid. This beam is designed to simulate the concrete pier of a dam and is anchored to the strong floor with threaded rods to ensure stability. The test configuration was tailored to fit the laboratory space, utilizing the strong floor for anchoring the reinforced concrete beam and an adjacent strong wall to secure two identical actuators that would apply the load. Each trunnion rod is outfitted with a permanent load cell at its dead end to monitor tension throughout the testing process.

Before testing commences, the rods are individually post-tensioned and balanced before load application through the actuators. Identical actuators are positioned on opposite sides of the reinforced concrete beam to apply equal loads to the rods via a built-up girder situated over the ends of all rods. This loading simulates the hydrostatic pressure exerted against the Tainter gate. **Error! Reference source not found.** illustrates the trunnion beam's rebar and ducts before the concrete pouring process. Figure 2 depicts the test configuration of the trunnion beam.



Figure 1: Trunnion beam's rebars and ducts prior to concrete pouring.



Figure 2: Trunnion beam's test configuration.

Before each test, all nine trunnion rods were individually tensioned to a specified percentage of the Guaranteed Ultimate Tensile Strength (GUTS) value, as illustrated in Figure 3. Care was taken to monitor the load cells attached to the dead ends of the rods to ensure that the tensions were balanced as closely as possible, aiming for a tolerance of approximately 0.5 kips. Figure 3 shows the trunnion rods' post-tensioning and load balancing prior to testing. Once all nine rods were balanced, the specified rod or rods were completely detensioned. This adjustment slightly alters the load distribution in the remaining rods before additional loads are applied.

Load was then applied through the actuators and attached girder in incremental steps of 87 kips, 122 kips, 160 kips, and 198 kips. These load levels were chosen to create a scenario where the load from the actuators approached the total post-tension load applied across all nine rods at 15% of GUTS. As the load in the actuators was increased to each specified value, the pressure was locked off, and all nine load cell readings were documented.

Thirty-five primary configurations and 22 secondary configurations were investigated. A comprehensive test matrix was developed, resulting in 57 configurations tested at 15% prestress and 35 configurations tested at 30%, 40%, 50%, and 60% of GUTS, culminating in 197 tests conducted.



Figure 3: Trunnion rods' post-tensioning and load balancing prior to testing.

We first considered a configuration where a single rod was detensioned to maximize available time, followed by another configuration involving the same detensioned rod and a second rod. Lastly, we performed a third test that included the first two rods and a third rod detensioned. For example, we detensioned Rod 1 and completed a load cycle, then conducted a test with Rod 1 and Rod 3 detensioned. Finally, we considered a third load cycle with Rod 1, Rod 3, and Rod 5 all detensioned. After completing these load cycles, all rods were rebalanced to the specified post-tension value, and two more trials of the same load cycles were considered to establish a statistical average. We conducted this procedure across dozens of possible configurations.

Post-tensioning was carried out, targeting a tension of 10% above the desired level. Tensions were balanced within 0.5 kips using load cells attached to the dead ends of the rods. Once balanced, the initial baseline tensions were recorded. The group of rods was then detensioned, and the new tensions were documented at a “0

psi” load from the actuator. The actuator was then loaded, with hydraulic pressure locked off at increments of 1200 psi, 1700 psi, 2200 psi, and 2700 psi, while load cell readings were recorded at each increment. After reaching and recording the maximum load at 2700 psi, the pressure in the system was released.

FINITE ELEMENT ANALYSES

A series of FE models was developed to validate the trunnion rod anchorage assembly test setup. The FE models were created using Abaqus/CAE 2023, as illustrated in Figure 4. The modeling framework utilized C3D8R linear hexahedral elements to accurately represent the trunnion rods, load beam, and anchorage plates. To enhance the accuracy of contact behavior, local mesh refinements were applied at the rod connection interfaces. The structural response of the assembly was simulated through a detailed five-step loading sequence, which included phases of rod pre-tensioning, stress redistribution, rod failure assessment, and the subsequent application of beam loads.

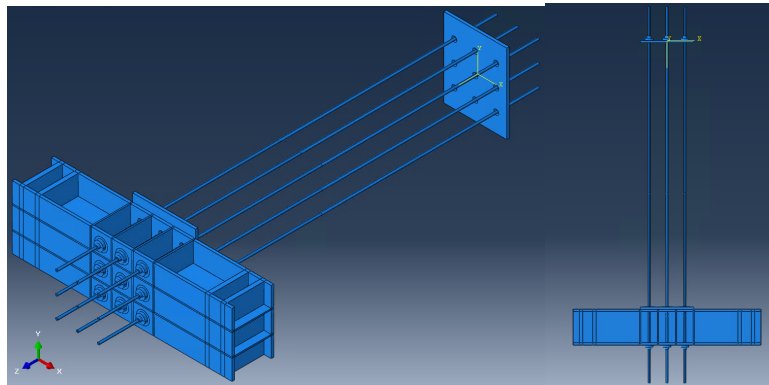


Figure 4: Trunnion rod anchorage assembly isometric and plane views.

Of the 197 laboratory-tested cases, 107 critical scenarios, including symmetric and asymmetric rod failures, were simulated using Abaqus FEA software. The mean absolute percent difference in the initial post-tension values from the FEA models, when compared to laboratory results, was found to be 6.86%. This value represents the averages of the 9 rods in the post-tensioned state, reflecting the conditions before any rods were detensioned. Consequently, the results pertain to the testing sequences at various post-tension percentages.

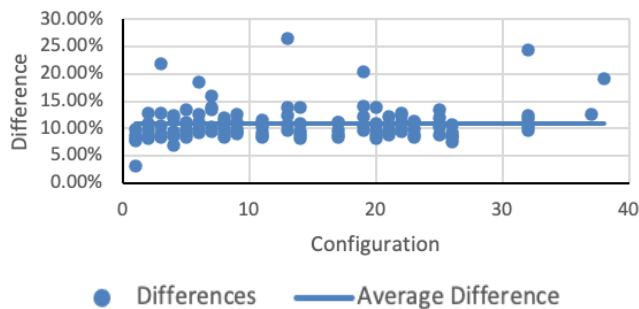


Figure 5: Differences of trunnion axial forces between the experimental tests and the FEA.

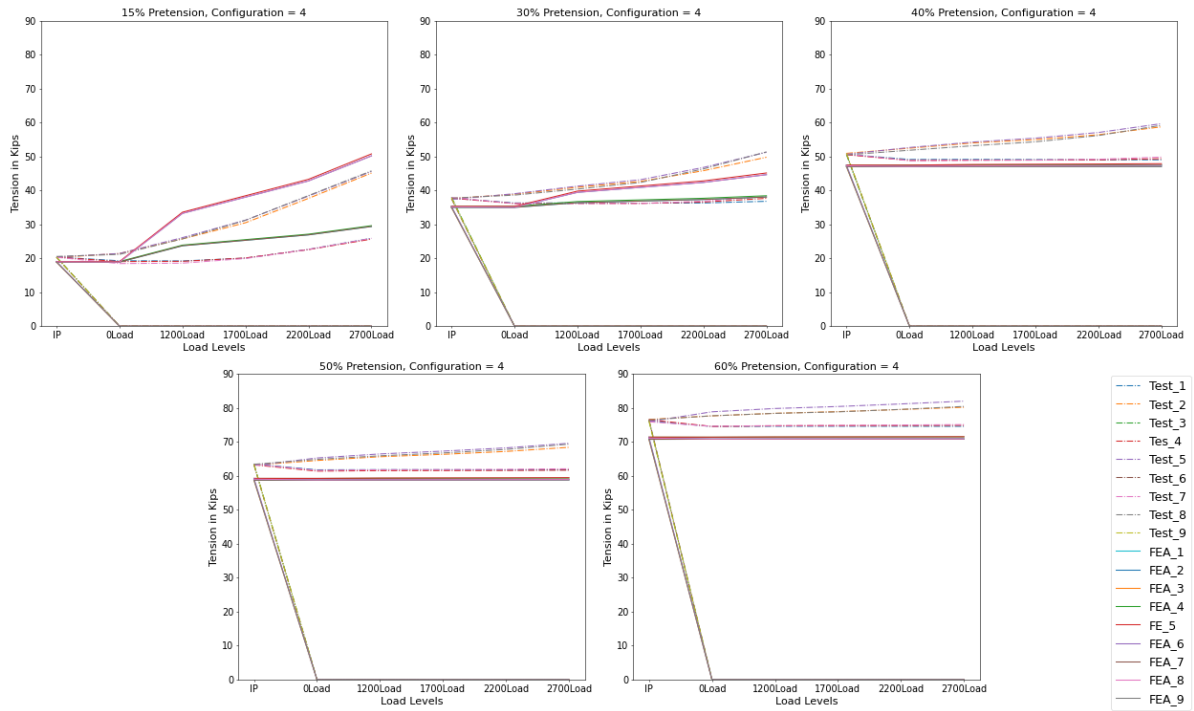


Figure 6: Typical comparison plot showing the Lab vs FEA tension levels in the rods for 15%, 30%, 40%, 50% and 60% post-tension test case.

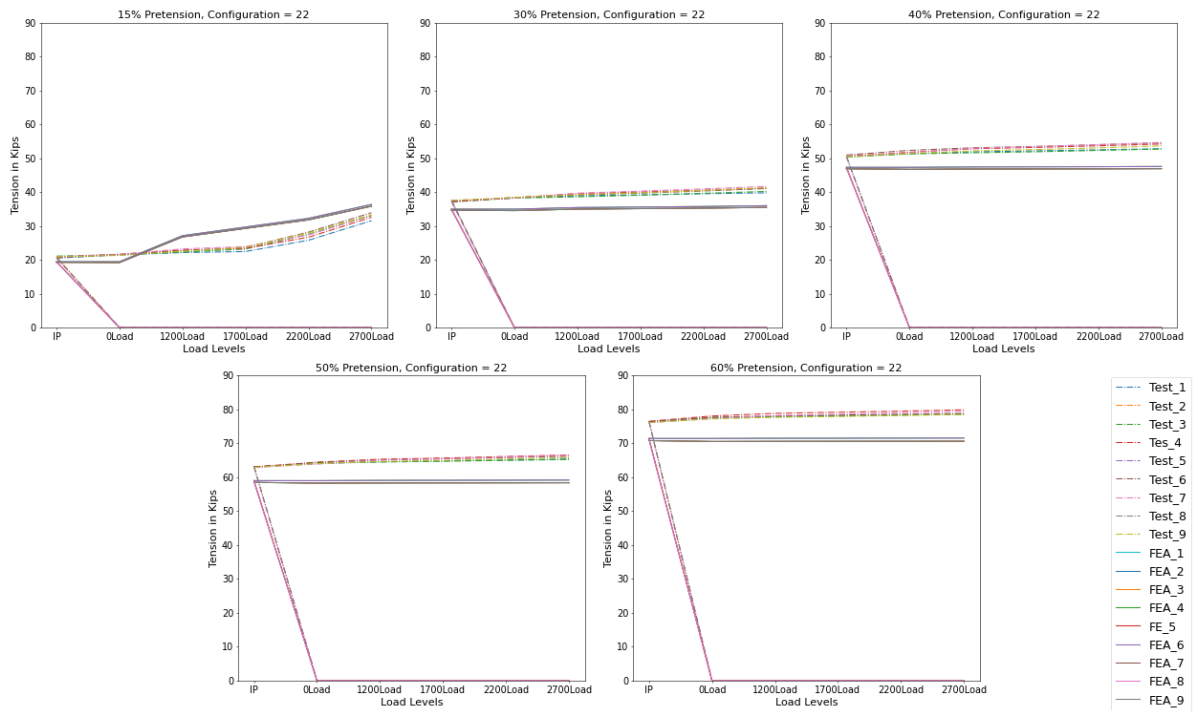


Figure 7: Typical Comparison plot showing the Lab vs FEA tension levels in the rods for 15%, 30%, 40%, 50% and 60% post-tension test case.

Additionally, Figure 5 summarizes the findings from comparing the final post-tension levels after applying approximately 200 kips of load using actuators. The analysis showed that the final post-tension levels from the FEA simulations had a mean absolute percent difference of 10.99% compared to the laboratory results.

Observations indicate that the applied load has the most significant impact on rod tension levels when the rods are post-tensioned to 15%, compared to other levels of post-tensioning. At 60% post-tensioning, the effect of the applied actuator load is minimal compared to what is observed at the 15% level. As a result, the most significant difference in tension levels between the laboratory rods and those in the FEA model is found at the 15% post-tension level. Figure 6 shows the configuration where rods #3, #5, and #9 are detensioned. This configuration represents the worst-case scenario due to considerable eccentricity resulting from an asymmetrical rod failure. In contrast, the configuration depicted in Figure 7, where rods #2, #5, and #8 are detensioned, is among the safest scenarios. In this case, the failure maintains the centroid of the anchorage system intact, resulting in unchanged risk levels.

CONCLUSIONS

An extensive parametric study included 107 finite element models, which varied in rod-failure and pre-tensioning configurations. The results demonstrated a high level of accuracy compared to laboratory findings, with a mean absolute percentage difference of 6.86% in initial post-tension levels and 10.99% in final post-tension levels. The findings indicate that post-tensioning at 15% is most sensitive to applied loads, while higher post-tension levels, such as 60%, exhibit minimal influence. Overall, the study confirms the FEA approach as a reliable predictive tool and supports its use in optimizing post-tensioning strategies for trunnion rod systems in bridge structures.

ACKNOWLEDGMENT

This project was sponsored by the Engineer Research and Development Center (ERDC) of the U.S. Army Corps of Engineers. We thank the ERDC-USACE for financial support under Cooperative Agreement W81EWF-20-SOI-0036 and appreciate the mentorship of Dr. Matthew Smith, ERDC's Technical Director for Water Resources Infrastructure Research and Development.

REFERENCES

1. O'Donnell, K.O. 1965. "Prestressed concrete anchorages for large Tainter gates," *In Proc., 10th Annual Convention of the Prestressed Concrete Institute, Precast/Prestressed Concrete Institute.*
2. Abela, C. M., and A. A. Abela, 2015. "Evaluation of an Existing Steel Box Trunnion Girder and Its Post-tensioned Anchors before Lift-off Testing: Case Study," *Practice Periodical on Structural Design and Construction*, 20(4), p.04014052.
3. Abela, C. M. 2017. "Evaluating Existing Passive Anchorage Systems for Tainter Gates," *ASCE Practice Periodical on Structural Design and Construction*, 23(1), p.04017032.
4. Zatar, W., Nghiem, H., Ray, J., Nguyen, H. and S. Anderson. 2023. Evaluating Post-Tensioned Trunnion Girders: A Comparative Study of Scale Model Tests and Numerical Analyses. Structural Health Monitoring, Final Report, ERDC.

5. Malik, H., and W. Zatar. 2019. "Software agents to support structural health monitoring (SHM)-informed intelligent transportation system for bridge condition assessment," IWSHM 2019, CA.
6. Malik, H., and W. Zatar. 2020. "Agent based routing approach to support structural health monitoring informed, intelligent transportation system," *Journal of Ambient Intelligence and Humanized Computing*, Volume 11, PP1031-1043.
7. Nguyen, H. Zatar W., and H. Mutsuyoshi. 2014. "Hybrid fiber-reinforced polymer girders topped with segmental precast concrete slabs for accelerated bridge construction," *Journal of the Transportation Research Record*, Volume 2407, issue 1, pp83-93.
8. Zatar W., and H. Nguyen. 2017. "Condition assessment of ground-mount cantilever weathering-steel overhead sign structures," *Journal of Infrastructure Systems*, Volume 23, Issue 4.
9. Zatar, W., Nguyen, H., and H. Nghiem. 2020. "Ultrasonic pitch and catch technique for non-destructive testing of reinforced concrete slabs," *Journal of Infrastructure Preservation and Resilience*, Volume 1, Issue 1, pp1-13.
10. AISC., 2016. Specification for structural steel buildings. ANSI/AISC, 360-16.